# Joining phenomena and joint strength of friction welded joint between pure aluminium and low carbon steel

**M. Kimura*[1], H. Ishii[2], M. Kusaka[1], K. Kaizu[1] and A. Fuji[3]**

This paper describes the joining phenomena and joint strength of friction welded joints between pure aluminium (P-Al) and low carbon steel (LCS) friction welds. When the joint was made at a friction pressure of 30 MPa with a friction speed of 27.5 $s^{-1}$, the upsetting (deformation) occurred at the P-Al base metal. P-Al transferred to the half radius region of the weld interface on the LCS side, and then it transferred toward the entire weld interface. When the joint was made at a friction time of 0.9 s, i.e. just after the initial peak of the friction torque, it had approximately 93% joint efficiency and fractured on the P-Al side. This joint had no intermetallic compound (IMC) at the weld interface. Then, the joint efficiency slightly decreased with increasing friction time. The joint had a small amount of IMC at the peripheral region of the weld interface when it was made at a friction time of 2.0 s. When the joint was made at a friction time of 0.9 s, the joint efficiency decreased with increasing forge pressure, and all joints were fractured at the P-Al side. Although the joint by forge pressure of 90 MPa had hardly softened region, it had approximately 83% joint efficiency. To clarify the fact of decreasing joint efficiency, the tensile strength of the P-Al base metal at room temperature was investigated, and the tensile test was carried out after various compression stresses and temperatures. The tensile strength of the P-Al base metal has decreased with increasing compression stress under any temperature. Hence, the fact that the joint did not achieve 100% joint efficiency was due to the decrease in the tensile strength of the P-Al base metal by the Bauschinger effect. To obtain higher joint efficiency and fracture on the P-Al side, the joint should be made without higher forge pressure, and with the friction time at which the friction torque reaches the initial peak.

Keywords: Friction welding, Pure aluminium, Low carbon steel, Joint efficiency, Initial peak, Intermetallic compound, Forge pressure, Bauschinger effect

## Introduction

Aluminium (Al) and many of its alloys are well-known materials that have highly attractive characteristics in terms of metallurgical and mechanical properties, e.g. high electrical and thermal conductivity, excellent corrosion resistance, and high specific strength. They are widely used for important structural components in automobiles, aerospace, and so on. On the other hand, fusion welds between Al and other metals such as steel,[1,2] copper,[1,3] and titanium[4] have poor mechanical properties due to the brittle intermetallic compound (IMC) layer produced at the joint interface. Moreover, fusion welds between Al or its alloys and various steels have some problems, e.g. generating of blowhole and cracking of the joint interface.[1] A welding process for joints between Al and other metals that will result in less degradation of the mechanical and metallurgical properties of the joint is therefore urgently required.

The solid state joining methods such as diffusion welding, friction welding, and so on, can be applied to join Al and other metals.[5] Many researchers have reported that the mechanical and metallurgical properties of friction welded joints between Al or its alloys and steel show desirable characteristics.[6-14] In addition, the friction welded joint between Al and steel was affected by the IMC that was generated at the weld interface and the joint had the brittle fracture of the joint occurring in the IMC.[12-14] However, the joining mechanism of friction welding between dissimilar materials such as Al and steel has not been fully clarified, so that the detail friction welding conditions have not been clarified. Furthermore, the joining mechanism between dissimilar materials differs from that of similar materials because mechanical properties such as the tensile strength and thermal properties such as the thermal conductivity are different in their combinations. To determine the friction welding conditions theoretically, it is necessary to clarify the joining phenomena.

In previous works,[15-21] we clarified the joining

[1]Department of Mechanical and System Engineering, Graduate School of Engineering, University of Hyogo, 2167 Shosha, Himeji, Hyogo 671-2280, Japan

[2]University of Hyogo, 2167 Shosha, Himeji, Hyogo 671-2280, Japan

[3]Department of Mechanical Engineering, National University Corporation–Kitami Institute of Technology, 165 Koen-cho, Kitami, Hokkaido, 090-8507, Japan

*Corresponding author, email mkimura@eng.u-hyogo.ac.jp

mechanism during the friction welding process for similar material joints. Then, we showed that the friction welded joints of several steels had 100% joint efficiency using only the first stage (up to the initial peak) of the friction process without adding forge pressure.[20,22-24] We also presented the friction welding condition for making several Al alloy joints with high joint efficiency.[21,25,26] If combinations of dissimilar materials such as Al and steel are joined by using the same method as in the previous reports,[15-26] the joining mechanism between them in friction welding will be clarified.

According to the background described above, the authors have been carrying out research for clarifying the joining mechanism between one base metal and another one in the friction process. In the present work, we investigate the joining phenomena during the friction process of friction welds between pure Al and low carbon steel. We also show the joint tensile strength under various friction welding conditions, especially the effects of friction time and forge pressure on the tensile strength of the joint.

## Experimental procedure

The materials used were commercially pure Al (type 1050-F, referred to as P-Al) and low carbon steel (referred to as LCS) in rods with a diameter of 16 mm. The chemical composition of P-Al was 0.06Si-0.15Fe-0.01Cu-0.00Mn-0.00Mg-0.00Zn-0.01Ti in mass%, the ultimate tensile strength was 115 MPa, the 0.2% yield strength was 113 MPa, and the elongation was 19%. The chemical composition of LCS was 0.13C-0.39Mn-0.21Si-0.19P-0.10S in mass%, the ultimate tensile strength was 448 MPa, the yield strength was 291 MPa, and the elongation was 35%. Those materials were machined to 12 mm in diameter of the weld faying (contacting) surface. The temperature changes during at the friction process at the centerline, half radius and periphery portions of the 1.0 mm longitudinal direction from the weld faying surface were measured by using the LCS specimen. The details of the specimen shape for measuring temperature change have been described in previous reports.[27,28] All weld faying surfaces of specimens were polished with a surface grinding machine before joining in order to eliminate the effect of surface roughness on the mechanical properties of dissimilar material joints.

A continuous (direct) drive friction welding machine was used for the joining. During friction welding operations, the friction speed and pressure were set to the following combinations: 27.5 $s^{-1}$ (1650 rpm) and 30 MPa. To observe the joining phenomena, we carried out three experimental methods as follows. The details of these methods have been described in previous reports.[15-28]

(1) The joining behaviour was recorded with a digital video camera. The friction torque was measured with a load-cell. The mineral insulated thermocouple with chromel-alumel was inserted into a drill hole of the LCS specimen for measuring temperature change. The friction torque and temperature were recorded with a personal computer through an A/D converter with a sampling time of 0.05 s.

(2) The fixed (steady) side chuck was directly connected to a hydraulic cylinder. The fixed side specimen was simultaneously and forcibly separated from the rotating side specimen when the friction time expired. The weld interface was separated at each friction time and observed.

(3) The fixed side specimen was fixed with an electromagnetic clutch. When the clutch was released, the relative speed between both specimens instantly decreased to zero. In this case, friction pressure could be maintained (loaded), so that the effect of deformation on the joint during the braking time would be negligible. As the braking time was smaller than 0.04 s, i.e. one rotation of the specimen, its effect was negligible.

In addition, the effect of friction time on the joint tensile strength was also investigated by using experimental method (3). All joint tensile test specimens were machined to 12 mm in diameter and 84 mm in parallel length. Vickers hardness distribution at the half radius location of the weld interface region on the P-Al side was measured with a load of 2.94 N (0.3 kgf) and that of the LCS side was measured with a load of 9.81 N (1 kgf). The measuring range was 6 mm from the weld interface, and the measuring interval was 100 μm. The weld interfaces after welding were analyzed using X-ray diffraction analysis. Moreover, the adjacent region of the weld interface of the as-welded joint was processed 3 mm in diameter and 3 mm in thickness by wire electric discharge machining for continuous *in situ* observation. The continuous *in situ* observation was carried out under the temperature of 723 K (450 ℃), and heat treated in a vacuum environment. A high temperature microscope was used to observe the IMC layer growth at the weld interface, which was recorded continuously using digital video. Analysis via Energy Dispersive X-ray Spectrometry (EDS) was carried out to analyze the chemical composition in the weld interface region. The detailed method of the *in situ* observation has been described in previous reports.[29,30]

## Results and Discussion

### Relationship between joining behaviour and friction torque

Figure 1a shows the joining behavior during friction process. Figure 1b shows the relationship between the friction time and the friction torque. Photos 1) to 5) are corresponding to the friction torque of (1) to (5) in Fig. 1, respectively. Photo 1) shows the state at the weld faying surfaces as they contacted each other, then the friction torque was increased. The P-Al side was slightly upset (deformed) as shown in photo 2), and then the friction torque reached the initial peak of (3). Thereafter, the upsetting and the flash (burr or collar) of P-Al increased with increasing friction time although the LCS side was not upset, as shown in photos 4) and 5).

### Temperature change during friction process

Figure 2 shows the relationship between the friction time and the temperature changes, in relation to friction torque during the friction process. The temperatures at the centerline, half radius and periphery portions on the weld interface of the LCS side were almost the same before the friction torque reached the initial peak. However, the difference in each temperature was approximately 50 K or less at a friction time of about 1.0 s or longer. Then, those temperatures reached approximately 723 K at a friction

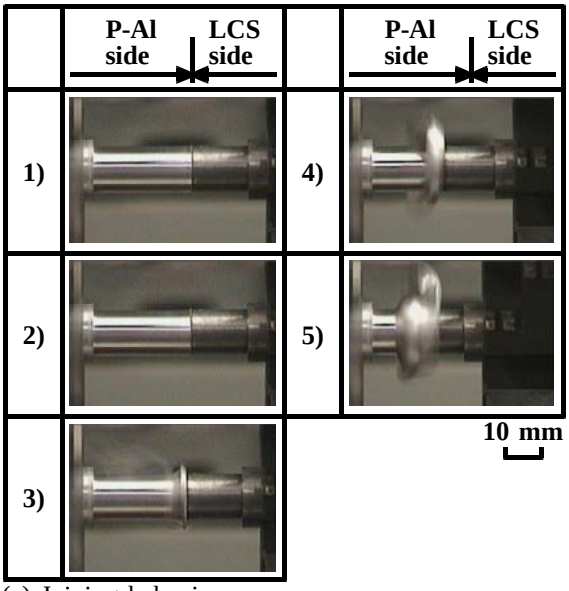


(a) Joining behaviour

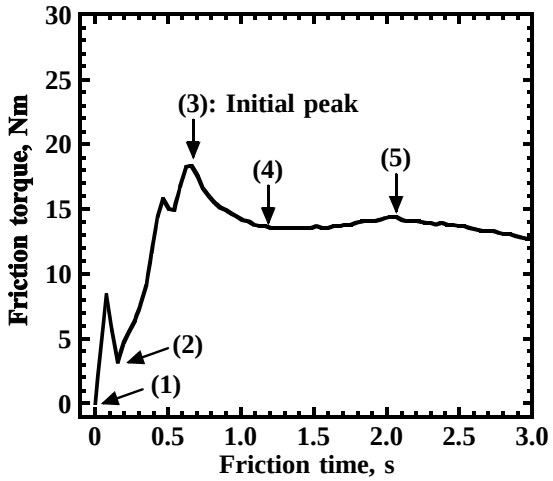


(b) Friction torque curve

1 Joining behaviour and friction torque curve during friction process

time of 2.0 s. That is, the temperature at the weld interface reached approximately 723 K or more after the initial peak under this friction welding condition. Incidentally, the temperature at the periphery portion was not measured after a friction time of about 2.2 s because the thermocouple was broken by the flash, which was exhausted from the P-Al side.

## Transitional changes of weld interface

Figure 3 shows examples of the appearances of the weld interfaces after welding. When a friction time was 0.04 s, i.e. both specimens had been rotated once, the weld interface on the P-Al side was slightly worn although the weld interface on the LCS side was similar before welding. When a friction time was 0.2 s, the concentric rubbing marks were observed around the half radius region of the weld interface on the P-Al side, and P-Al transferred to a similar region of the weld interface on the LCS side. The concentric rubbing marks on the P-Al side were extended, and the transferred P-Al on the LCS side increased with increasing friction time (0.5 s). When a friction time was 0.9 s, i.e. just after the initial peak, the

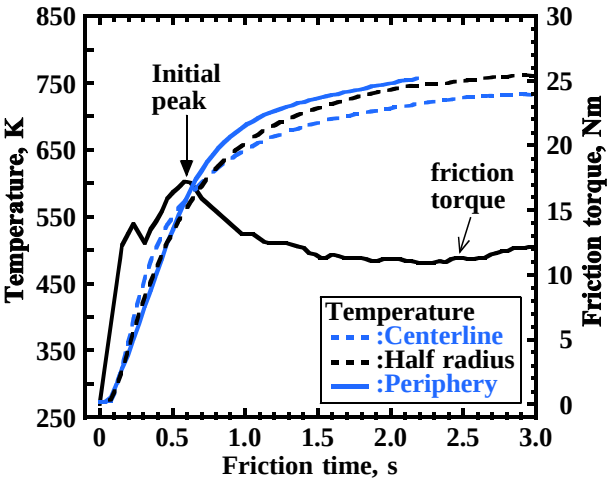


2 Relationship between friction time and temperature changes, in relation to friction torque during friction process

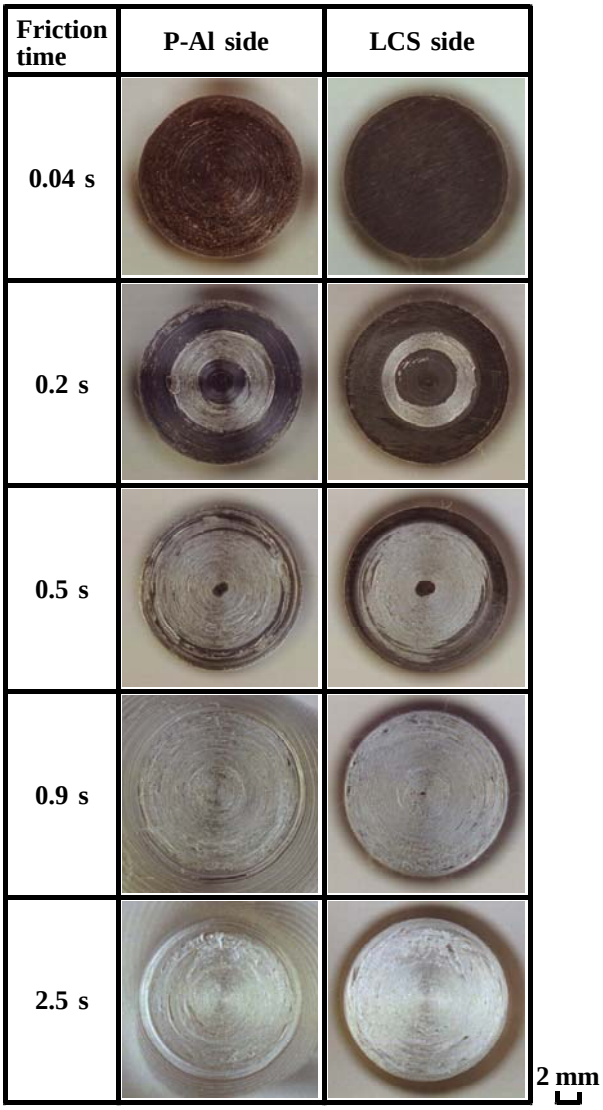


3 Appearances of weld interfaces after welding

flash on the P-Al side was increased, and P-Al transferred to the entire weld interface on the LCS side. Then, the P-Al flash increased with increasing friction time, whereas

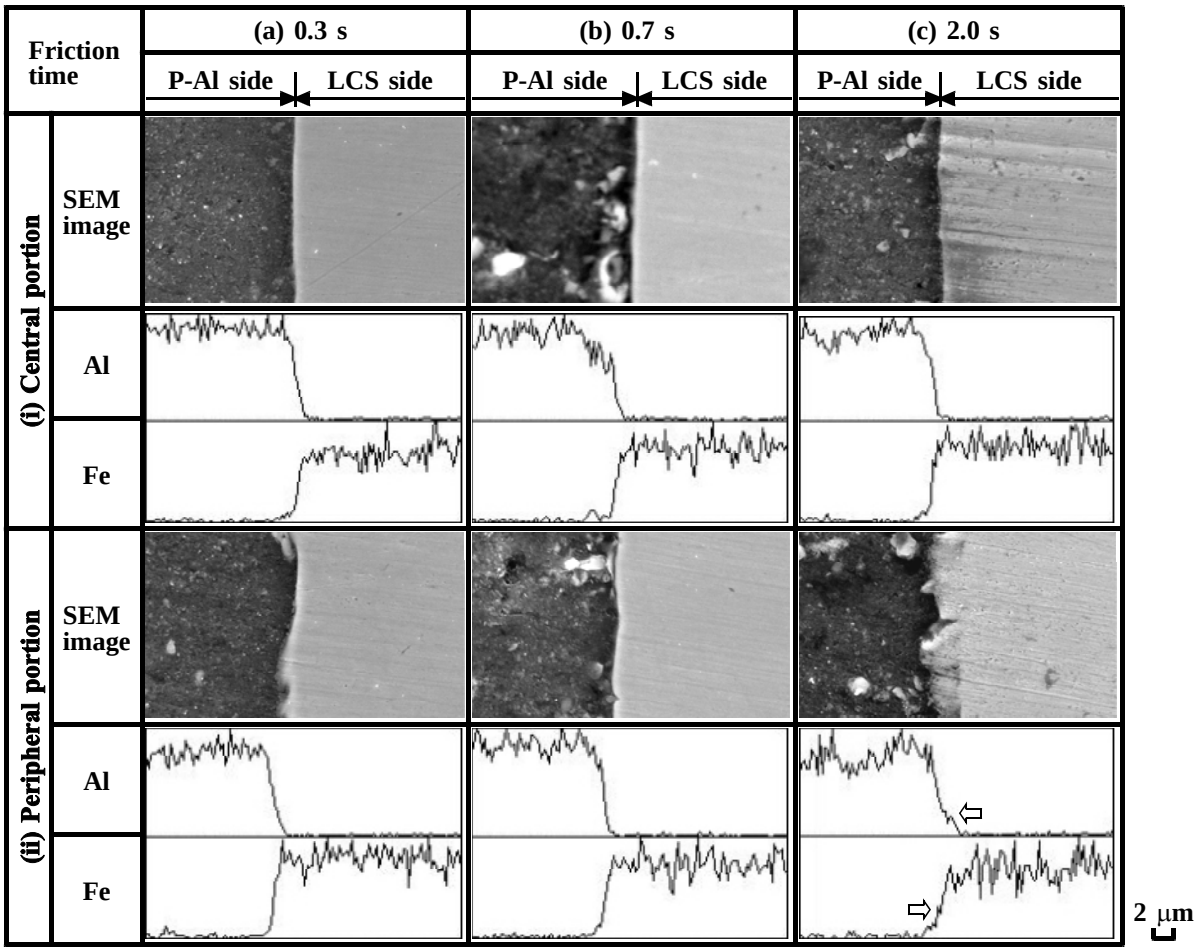


4 SEM images and EDS analysis results of (i) central and (ii) peripheral portions at weld interface region; friction time of (a) 0.3, (b) 0.7, and (c) 2.0 s

the LCS side was not deformed (2.5 s). In this connection, the peak of the IMC pattern between Al and Fe of those weld interfaces was not detected on those surfaces by X-ray diffraction analysis.

## Observation of weld interface region

Figure 4 shows the SEM images and EDS analysis results of the central and peripheral portions at the weld interface region at friction times of 0.3, 0.7, and 2.0 s. In this case, forge pressure was applied at an identical friction pressure, i.e. 30 MPa. The central and peripheral portions of the weld interfaces were clear and an IMC layer was not observed at a friction time of 0.3 s (a in Figs. 4i and 4ii). Also, the distribution lines corresponding to Al and Fe by EDS analysis had no plateau part at the weld interface. The joint at a friction time of 0.7 s was similar to the joint of 0.3 s (b in Figs. 4i and 4ii). However, the peripheral portion of the weld interface was not clear although the central portion was clear, when a friction time was 2.0 s (c in Figs. 4i and 4ii). In addition, the distribution lines of Al and Fe had small plateau parts at the adjacent region of the weld interface, which are indicated by arrows (c in Fig. 4ii). The composition of this region was approximately 73Al-27Fe in at.% and it was corresponded to $Fe_2Al_5$ or $FeAl_3$. That is, the IMC was generated at the peripheral portion of the weld interface when the joint was made with a friction time of 2.0 s.

To clarify the IMC in detail, the continuous *in situ* observation of the interlayer growth at the weld interface of the joint was carried out. Figure 5 shows the microstructures at the half radius portion of the weld interface region of the joint during post-weld heat treatment (PWHT). In this case, the as-welded joint was made at a friction time of 0.7 s (close to the initial peak) with forge pressure of 30 MPa. One of the pictures was the as-welded condition (Fig. 5a), and the other was the condition for heating time of 172.8 ks (48 hours) after (Fig. 5b). The heating temperature was 723 K, which was determined from the result of Fig. 2. The weld interface of the as-welded had no IMC layer, as shown in Fig. 5a. However, the weld interface had an IMC layer with a width of about 2 μm through PWHT and that grew to the P-Al side from the LCS side, as shown in Fig. 5b. Figure 6 shows the SEM image at the half radius portion of the weld interface region through PWHT with heating temperature of 723 K and a heating time of 259.2 ks (72 hours). The IMC layer was observed clearly, and its width was about 55 μm. The composition of IMC was approximately 72Al-28Fe in at.%, and it corresponded to $Fe_2Al_5$ or $FeAl_3$. The composition of IMC with PWHT corresponded to that of the joint with a friction time of 2.0 s. Hence, the weld interface had generated the IMC layer when the joint was made with long friction time.

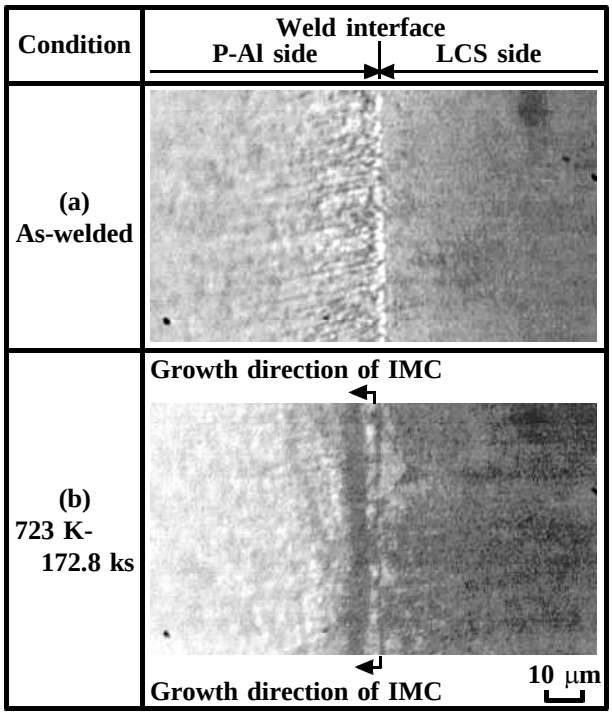


5 Microstructures at half radius portion of weld interface region of joint at friction time of 0.7 s during PWHT; (a) as-welded and (b) heating temperature of 723 K with heating time of 172.8 ks

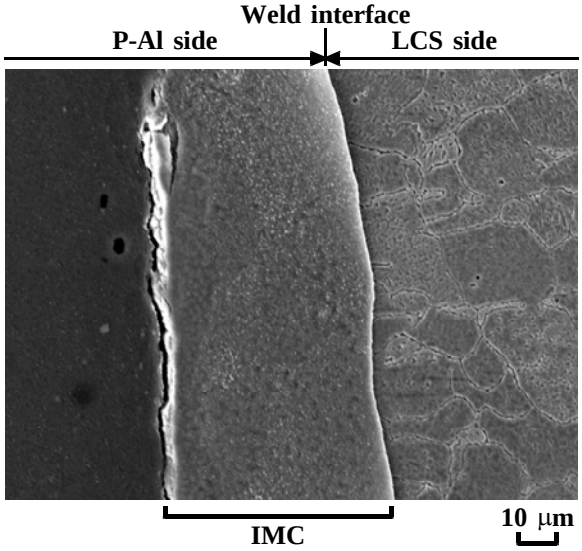


6 SEM image at half radius portion of weld interface region of joint at friction time of 0.7 s after PWHT; heating temperature of 723 K and heating time of 259.2 ks

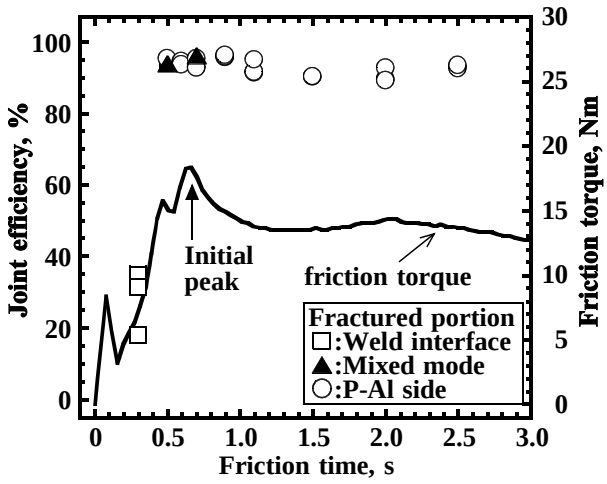


7 Relationship between friction time and joint efficiency of joint, in relation to friction torque

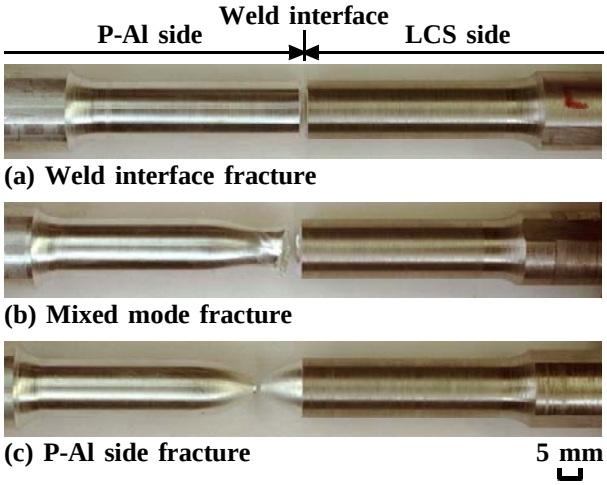


8 Appearances of joint tensile test specimens after tensile testing

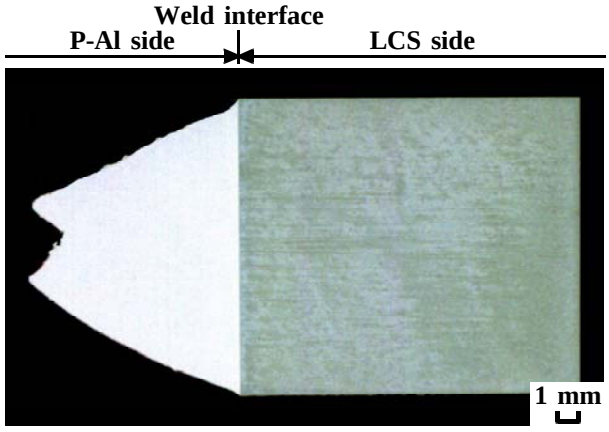


9 Cross-sectional appearance of fractured specimen of joint with P-Al side fracture after tensile testing

## Joint efficiency

Figure 7 shows the relationship between the friction time and the joint efficiency of the joint, plotted alongside the friction torque curve. The joint efficiency was defined as the ratio of the joint tensile strength to the ultimate tensile strength of the P-Al base metal. Figure 8 shows the appearances of the joint tensile test specimens after tensile testing. In this case, forge pressure was applied at an identical friction pressure, i.e. 30 MPa. The joint efficiency at a friction time of 0.3 s was approximately 28%. The joint fractured at the weld interface, which had a little P-Al adhering to the LCS side interface, as shown

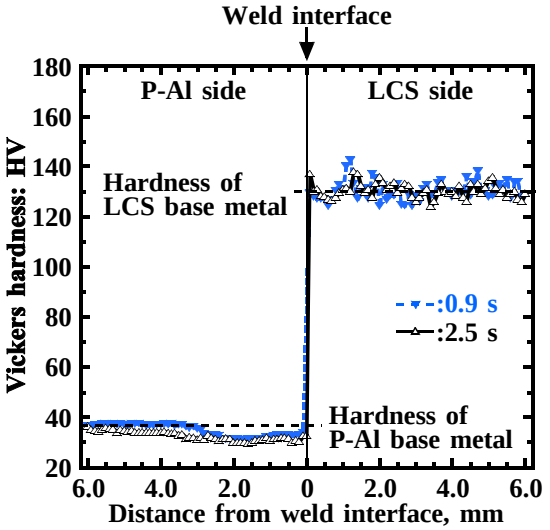


10 Vickers hardness distribution across weld interface at half radius location of joint; friction time of 0.9 and 2.5 s

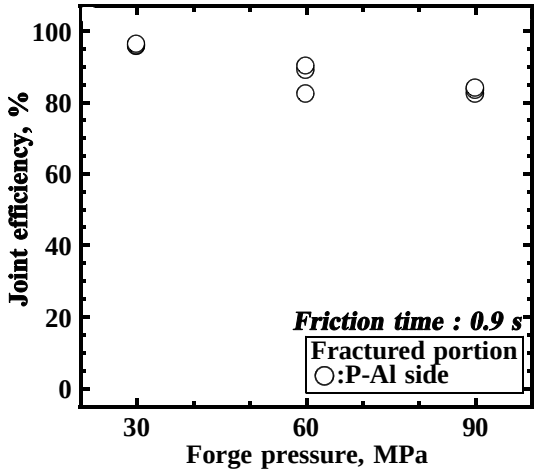


11 Relationship between forge pressure and joint efficiency of joint at friction time of 0.9 s

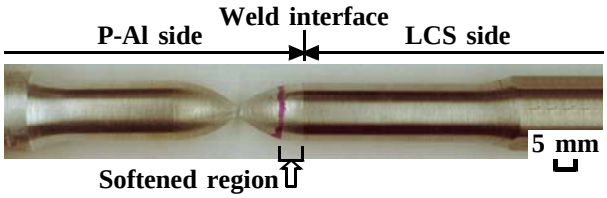


12 Appearance of joint tensile test specimen with P-Al side fracture after tensile testing; friction time of 0.9 s and forge pressure of 90 MPa

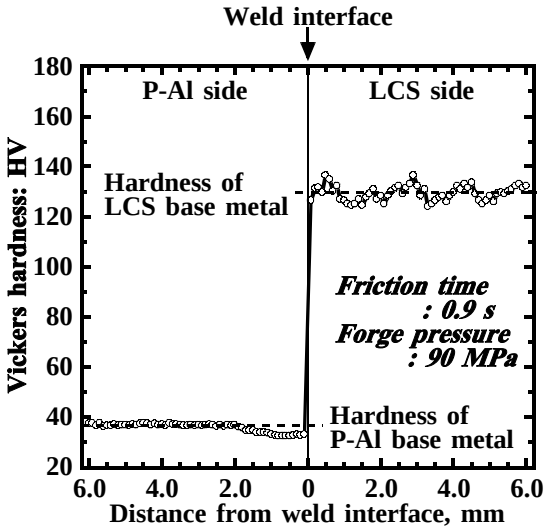


13 Vickers hardness distribution across weld interface at half radius location of joint; friction time of 0.9 s and forge pressure of 90 MPa

in Fig. 8a. That is, a sufficient quantity of heat for welding could not be produced during this friction time (0.3 s). The joint efficiency increased with increasing friction time, and then it was approximately 94% at a friction time of 0.5 s. Almost all joints fractured between the P-Al side and the weld interface (mixed mode fracture), as shown in Fig. 8b, although one of the joints fractured from the P-Al side as shown in Fig. 8c. The joint had approximately 96% joint efficiency at a friction time of 0.9 s, i.e. just after the initial peak, and P-Al transferred to the entire weld interface on the LCS side. All joints fractured from the P-Al side. In addition, this joint efficiency was the maximum value obtained in the present experiments. Thereafter, the joint efficiency slightly decreased with increasing friction time after the friction torque reached the initial peak, although all joints fractured from the P-Al side. Figure 9 shows the cross-sectional appearance of the fractured specimen with the P-Al side fracture after tensile testing. The weld interface had neither a not-joined region nor defects such as cracking. That is, P-Al and LCS were tightly joined. Figure 10 shows the Vickers hardness distribution across the weld interface at the half radius location of the joint at friction times of 0.9 and 2.5 s. The joint at a friction time of 0.9 s had a softened region that extended about 3 mm in the longitudinal direction of the P-Al side. The softened region extended toward the measured line in the longitudinal direction of the P-Al side at a friction time of 2.5 s. Hence, the joint did not achieve 100% joint efficiency by the softening of the adjacent region of the weld interface on the P-Al side. However, these joints fractured from the P-Al side.

## Influence of forge pressure

Generally speaking, forge pressure will be able to reduce the extent of a softened region from the joint and to improve the joint efficiency.[9,31-37] In an attempt to push out a softened region on the P-Al side, the effect of forge pressure on joint efficiency was investigated. Figure 11 shows the relationship between the forge pressure and the joint efficiency of the joints. Figure 12 shows the appearances of the joint tensile test specimens after tensile testing. In this case, a friction time was set to 0.9 s because the joint efficiency had the maximum value, as shown in Fig. 9. These joints were made by experimental method (3). Also, the forge pressures were set to within the yield strength of the P-Al base metal. The joint efficiency decreased with increasing forge pressure, and it was approximately 83% at a forge pressure of 90 MPa. In

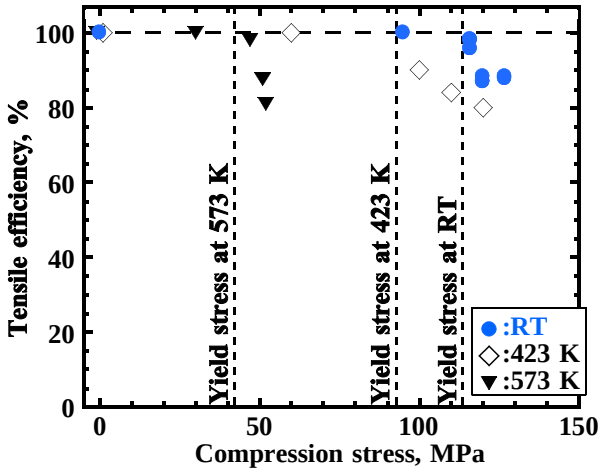


14 Relationship between compression stress and tensile efficiency of P-Al base metal under various temperatures

addition, all joints fractured from the P-Al side and the weld interface had no defect such as cracking, as shown in Fig. 12. Figure 13 shows the Vickers hardness distribution across the weld interface at the half radius location of the joint at a forge pressure of 90 MPa. The joint had a softened region that extended about 2 mm in the longitudinal direction of the P-Al side. The softened region of this joint was narrower than that of a forge pressure of 30 MPa, as shown in Fig. 10. Moreover, the fractured portion of this joint was not the softened region but the P-Al base metal because the rupture occurred on the P-Al side with the LCS side away from the edge of the softened region, which is indicated by arrows, which is indicated by arrows as shown in Fig. 12. Hence, the joint fractured from the P-Al base metal although it did not achieve 100% joint efficiency. This result differed from many results of friction welded joints between dissimilar materials.[9,31-37] On the other hand, the tensile strength of the friction welded joints such as Al-alloy/Copper[36] and Copper/Steel[37] decreased with increasing forge pressure. That is, several friction welded joints made with higher forge pressure were fractured from the base metal although those joints did not achieve 100% joint efficiency. Although the difference in the anisotropic properties of the base metal between the longitudinal and radial directions was clarified,[25] the reason why the joint did not achieve 100% joint efficiency was not clarified in detail.

To clarify the reason why the joint did not achieve 100% joint efficiency, the tensile strengths of the P-Al base metal with adding various compression stresses were investigated. This material was machined to 12 mm in diameter and 12 mm in parallel length to prevent buckling for the parallel part of the tensile test specimen during compression loads. The tensile test specimen was set to the tensile testing machine with the electric furnace, which was processed under various compression loads and temperatures. Then, the specimen was remachined to 12 mm in diameter to the parallel part of it after compression. Thereafter, the tensile test was carried out under room temperature. Figure 14 shows the relationship between the compression stress and the tensile efficiency of the P-Al base metal at various temperatures. The tensile efficiency was defined as the ratio of the tensile strength to the ultimate tensile strength of the P-Al base metal with no compression loads under each temperature. When the compression stress was higher than the yield stress of the P-Al base metal at room temperature, tensile efficiency did not reach 100%, which is indicated by solid circle symbols. The tensile efficiency decreased with increasing compression stress when it was higher than the yield stress at 423 K (150 ℃), which is indicated by open rhombus symbols. Moreover, when the P-Al base metal was softened by temperature of 573 K (300 ℃), the tensile efficiency also decreased with increasing compression stress when it was higher than the yield stress, which is indicated by solid inverted delta symbols. That is, the tensile efficiency was lower when the compression stress was higher than the yield stress of the P-Al base metal at each temperature. Consequently, the joint did not achieve 100% joint efficiency because the tensile strength of the P-Al base metal was decreased by higher compression stress. It was considered that the decrease in the tensile strength of the P-Al base metal by higher compression stress was due to the Bauschinger effect. The fact that the joint did not achieve 100% joint efficiency was due to the decrease in the tensile strength of the P-Al base metal by the Bauschinger effect, although further investigation is necessary to elucidate the detailed mechanical properties of the joints. Hence, to obtain higher joint efficiency and fracture on the P-Al side, the joint should be made with the opportune value without higher forge pressure, and with the friction time at which the friction torque reaches the initial peak.

## Conclusions

This report described the joining phenomena and joint strength of a friction welded joint between commercially pure aluminium (P-Al) and low carbon steel (LCS). In particular, we investigated the joining phenomena during the friction process, and the joint tensile strength of the joint under various friction welding conditions such as friction time and forge pressure. The following conclusions are provided.

1. When the joint was made at a friction pressure of 30 MPa and a friction speed of 27.5 $s^{-1}$, the upsetting (deformation) occurred at the P-Al base metal. P-Al at the half radius region of the weld interface transferred on the LCS side, and then it transferred toward the entire weld interface.

2. When the joint was made with a friction time of 0.9 s, i.e. just after the initial peak of the friction torque, it had approximately 93% joint efficiency and fractured at the P-Al side. This joint had no intermetallic compound (IMC) at the weld interface according to SEM observation level. Then, the joint efficiency slightly decreased with increasing friction time.

3. The joint had a small amount of IMC at the weld interface when it was made at a friction time of 2.0 s. The IMC layer grew to the P-Al side from the LCS side, and it corresponded to $Fe_2Al_5$ or $FeAl_3$ by EDS analysis.

4. The joint efficiency decreased with increasing forge pressure, and all joints were fractured on the P-Al side when a friction time was 0.9 s. Although the joint by forge pressure of 90 MPa had hardly softened region, it had approximately 83% joint efficiency.

5. The tensile strength of the P-Al base metal decreased with increasing compression stress under any temperature

when the compression stress was higher than the yield stress of the P-Al base metal. Hence, the fact that the joint did not achieve 100% joint efficiency was due to the decrease in the tensile strength of the P-Al base metal by the Bauschinger effect.

In conclusion, to obtain higher joint efficiency and fracture on the P-Al side, the joint should be made without higher forge pressure, and with the friction time at which the friction torque reaches the initial peak.

## Acknowledgements

This research was partially supported by the Ministry of Education, Culture Sports, Science and Technology, Grant-in-Aid for Young Scientists (B), 20760496, 2008. We wish to thank the staff members of the Machine and Workshop Engineering at the Graduate School of Engineering, University of Hyogo.

## References

1. Technical Committee on Structural Transition Joint: *J. Light Metal Welding & Construction*, 1978, **16**, (8), 345-364 (in Japanese).
2. Y. Ueda and M. Niinomi: *J. Jpn. Inst. Met.*, 1978, **42**, (6), 543-549 (in Japanese).
3. R. J. C. Dawson: *Welding Research Council Bulletins*, 1983, WRC Bulletin 287, 1-17.
4. The Japan Titanium Society: "Titanium", 268-269; 2007, Tokyo, Kogyo Chosakai Publishing (in Japanese).
5. M. Maalekian: *Sci. Technol. Weld. Joining*, 2007, **12**, (8), 738-759.
6. Americaan Welding Society: "WELDING HANDBOOK, Eighth Edition, Vol. 2", 750; 1991, Miami, Americaan Welding Society.
7. S. Elliott and E. R. Wallach: *Met. Constr.*, 1981, **13**, (4), 221-225.
8. H. Ochi, K. Ogawa, Y. Yamamoto and Y. Suga: *J. Jpn. Soc. Fract. Strength Mater.*, 1994, **28**, (4), 143-154 (in Japanese).
9. H. Tokisue and K. Katoh: *J. Jpn. Inst. Light Met.*, 2002, **52**, (8), 378-383 (in Japanese).
10. W. B. Lee, Y. M. Yeon, D. U. Kim and S. B. Jung: *Mater. Sci. Technol.*, 2003, **19**, 773-778.
11. M. Yilmaz, M. Çöl and M. Acet: *Mater. Charact.*, 2003, **49**, 421-429.
12. N. Yamamoto, M. Takahashi, M. Aritoshi and K. Ikeuchi: *Q. J. Jpn. Weld. Soc.*, 2005, **23**, (2), 352-358 (in Japanese).
13. N. Yamamoto, M. Takahashi, M. Aritoshi and K. Ikeuchi: *Q. J. Jpn. Weld. Soc.*, 2005, **23**, (3), 496-503 (in Japanese).
14. N. Yamamoto, M. Takahashi, M. Aritoshi and K. Ikeuchi: *Q. J. Jpn. Weld. Soc*., 2005, **23**, (4), 622-627 (in Japanese).
15. M. Kimura, H. Mioh, M. Kusaka, K. Seo and A. Fuji: *Q. J. Jpn. Weld. Soc*., 2002, **20**, (3), 425-431 (in Japanese).
16. M. Kimura, M. Kusaka, K. Seo and A. Fuji: *Q. J. Jpn. Weld. Soc.*, 2002, **20**, (3), 432-438 (in Japanese).
17. M. Kimura, M. Kusaka, K. Seo and A. Fuji: *Q. J. Jpn. Weld. Soc*., 2002, **20**, (4), 559-565 (in Japanese).
18. M. Kimura, Y. Ohtsuka, G. B. An, M. Kusaka, K. Seo and A. Fuji: *Q. J. Jpn. Weld. Soc*., 2003, **21**, (4), 615-622 (in Japanese).
19. M. Kimura, G. B. An, M. Kusaka, K. Seo and A. Fuji: *Q. J. Jpn. Weld. Soc*., 2005, **23**, (3), 460-468 (in Japanese).
20. M. Kimura, M. Kusaka, K. Seo and A. Fuji: *JSME Int. J.(Series A)*, 2003, **46**, (3), 384-390.
21. M. Kimura, M. Kusaka, K. Seo and A. Fuji: *Sci. Technol. Weld. Joining*, 2005, **10**, (3), 378-383.
22. M. Kimura, M. Kusaka, K. Seo and A. Fuji: Proc. 57th Assembly of IIW, Osaka, Japan, July 2004, International Institute of Welding, Doc. III-1290-04, 139-149.
23. M. Kimura, Y. Ohtsuka, M. Kusaka, K. Seo and A. Fuji: *Q. J. Jpn. Weld. Soc*., 2005, **23**, (4), 577-586 (in Japanese).
24. M. Kimura, M. Kusaka, K. Seo and A. Fuji: *JSME Int. J.(Series A)*, 2005, **48**, (4), 399-405.
25. M. Kimura, M. Choji, M. Kusaka, K. Seo and A. Fuji: *Sci. Technol. Weld. Joining*, 2005, **10**, (4), 406-412.
26. M. Kimura, M. Choji, M. Kusaka, K. Seo and A. Fuji: *Sci. Technol. Weld. Joining*, 2006, **11**, (2), 209-215.
27. M. Kimura, M. Kusaka, K. Kaizu and A. Fuji: *J. Solid Mech. Mater. Eng.*, accepted.
28. M. Kimura, K. Kasuya, M. Kusaka, K. Kaizu and A. Fuji: *Sci. Technol. Weld. Joining*, accepted.
29. A. Fuji: *Sci. Technol. Weld. Joining*, 2002, **7**, (6), 413-416.
30. A. Fuji, K. Ikeuchi, Y. S. Sato and H. Kokawa: *Sci. Technol. Weld. Joining*, 2004, **9**, (6), 507-512.
31. M. Aritoshi, K. Okita, T. Enjo and K. Ikeuchi: *Q. J. Jpn. Weld. Soc*., 1988, **6**, (1), 16-22 (in Japanese).
32. M. Futamata and A. Fuji: *Q. J. Jpn. Weld. Soc*., 1989, **7**, (4), 432-438 (in Japanese).
33. A. Fuji, K. Ameyama, H. Kokawa, Y. Satoh and T. H. North: *Sci. Technol. Weld. Joining*, 2001, **6**, (1), 23-30.
34. W. B. Lee and S. B. Jung: *Mater. Trans.*, 2004, **45**, (9), 2805-2811.
35. H. Ochi, K. Ogawa, Y. Yamamoto and Y. Suga: *J. Jpn. Inst. Light Met.*, 1997, **47**, (6), 347-351 (in Japanese).
36. H. Ochi, K. Ogawa, Y. Yamamoto, G. Kawai and T. Sawai: *Q. J. Jpn. Weld. Soc*., 2003, **21**, (3), 381-388 (in Japanese).
37. W. B. Lee and S. B. Jung: *Z. Metallku.*, 2003, **94**, (12), 1300-1306.